Available online at www.sciencedirect.com

SciVerse ScienceDirect

Ceramics International 39 (2013) 7507–7515

CERAMICS INTERNATIONAL

www.elsevier.com/locate/ceramint

Slag conditioning effects on MgO–C refractory corrosion performance

A.P. Luz[a,*], F.C. Leite[b], M.A.M. Brito[c], V.C. Pandolfelli[a]

[a]Federal University of São Carlos, Materials Engineering Department, Rod. Washington Luiz, km 235, São Carlos, SP 13565-905, Brazil

[b]ArcelorMittal Monlevade, Technical Management and Production Planning, Av. Getúlio Vargas, 100, João Monlevade, MG 35930-900, Brazil

[c]Magnesia Refratários S.A., Research and Development Center, Praça Louis Ensch, 240, Contagem, MG 32210-900, Brazil

Received 24 February 2013; received in revised form 28 February 2013; accepted 1 March 2013
Available online 14 March 2013

Abstract

Slag conditioning practice provides important benefits to the steelmaking processes including ladle refractory life improvement, lower flux cost/additions, better control of metal recovery, among others. Furthermore, with the advent of thermodynamic and mass balance calculations it is possible to predict the slag saturation and define the most suitable conditioner (oxide components) that should be added during the operational process. Thus, the aim of this work was to analyze the interaction of industrial slags and a MgO–C refractory composition by thermodynamic simulations (FactSage™). Based on the attained results, a conditioned slag was designed and corrosion tests in the laboratory were carried out (cup-tests and induction furnace), for two MgO–C materials containing distinct magnesia sources. According to the calculated slag penetration area and refractory corrosion rate, a remarkable enhancement of the MgO–C bricks wear resistance was observed when such materials were placed in contact with the conditioned molten slag. Therefore, proper slag engineering can be a suitable replacement for purchased synthetic slags and the conditioning practices can directly improve refractory life, with more competitive costs for both, refractory producers and end-users.

Keywords: C. Corrosion; Slag; Refractory; Thermodynamic calculations

1. Introduction

Slag is an important component in iron and steelmaking operations due to its close contact with metal, refractories and furnace atmosphere. Usually, they are solid solutions consisting of molten metal oxides and fluorides floating on the top of the steel [1–2]. The main functions of this molten liquid in the steel production are [1–5]: (1) cover the electrodes in the electric (EAF) and ladle (LF) furnaces, inhibiting their oxidation and protecting the refractories from thermal radiation; (2) improve the quality of the steel by absorbing deoxidation products and inclusions; (3) dephosphorize the metal bath in the electric furnace and desulfurize it in the ladle; (4) protect the metal from oxidation, and nitrogen and hydrogen pick-up; and (5) minimize heat loss.

"Slag engineering" or the good slag practice [based on the optimum balance between the refractory oxides (CaO and MgO) and the fluxing components (SiO_2, Al_2O_3, CaF_2, and iron oxide)] is becoming an essential issue in many companies, due to the increasing necessity faced by the end-users to cut costs and produce high quality steel [3,5,6].

The goal of ladle refining is to deliver homogeneous liquid steel to the caster (or ingot station) at the right temperature, time, and attaining the chemical specifications [1]. Usually, this is only achieved when the slag is conditioned and optimized. A suitable slag can be defined as a liquid presenting enough viscosity at a high temperature to allow the required slag–metal interactions, but not too fluid in order to attack the refractory lining.

Considering that most refractory materials applied in the ladles' slag line are MgO–C bricks [1,6,7], one of the crucial aspects to minimize slag attack during the operational process of such equipment is to adjust the liquid composition in order to attain dual saturation (with respect to CaO–MgO) or at least the MgO one. The MgO content required for liquid saturation is a function of the slag basicity and temperature [2,8,9]. Nevertheless, with the advent of thermodynamic and mass

*Corresponding author. Tel.: +55 16 33518253; fax: +55 16 33615404.
E-mail address: anapaula.light@gmail.com (A.P. Luz).

0272-8842/$ - see front matter © 2013 Elsevier Ltd and Techna Group S.r.l. All rights reserved.
http://dx.doi.org/10.1016/j.ceramint.2013.03.001

balance calculations [8,10,11], it is possible to predict the slag saturation level, its overall chemical composition and define the most suitable conditioner (oxide components) that should be added during the ladle operation. The slag mass balance models are commonly based on phase equilibrium diagrams data using statistical and mathematical approaches to describe the *liquidus* phase relations as a function of temperature and composition (i.e., as illustrated in Fig. 1, for basic slags that are compatible with basic refractories) [1,11].

Fluorine-based fluxes are commonly added to slags as [12]: (1) they decrease the melting point of the compositions, so that a liquid with higher basicity (with greater content of refractory oxides, i.e., MgO and CaO) can be used, and (2) they reduce the liquid viscosity. CaF_2 and MgF_2 are the most usual fluorides added during the ladle operation process and they act by breaking up the silicate network of the molten slag, as presented below [1,12]:

$$\equiv Si-O-Si\equiv + F^- \rightarrow \equiv SiO^- + F-Si\equiv \quad (1)$$

Although the addition of CaF_2 and MgF_2 has a positive effect on the liquid features, it also affects the refractory lining wear by inducing a greater liquid penetration, consequently, speeding up the slag-refractory chemical reactions [12].

Considering these aspects, this work addresses the analysis of the interaction of some industrial ladle slags (containing CaF_2) and MgO–C refractory compositions. Firstly, the chemical reactions and phase transformations involved in the refractory-slag contact at high temperature were carried out by thermodynamic simulations (FactSage™). Based on the attained results, the most reactive slag was selected and a conditioned composition was designed, prepared and experimentally tested in laboratorial corrosion tests [static (cup tests) and dynamic measurements (induction furnace)] in order to evaluate the changes or benefits induced by the conditioning practice for MgO–C bricks. Physical, thermo-mechanical (apparent porosity, cold crushing strength, hot modulus of rupture and thermal shock resistance), and microstructural characterization (SEM and EDS analyses) of the evaluated refractory materials were also carried out.

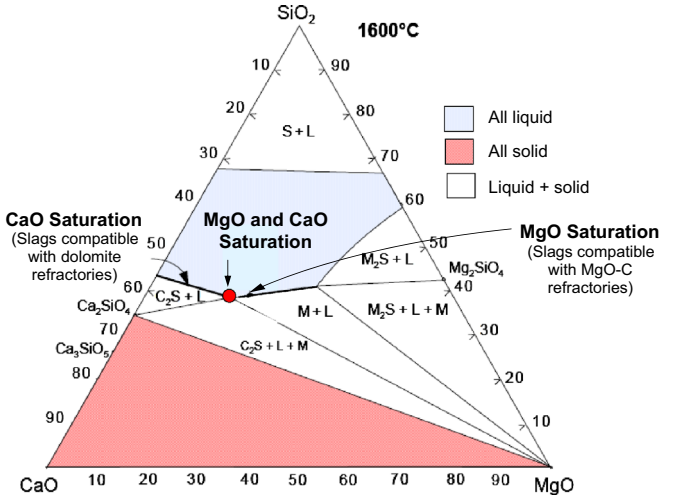

Fig. 1. Phase equilibrium diagram of the CaO–MgO–SiO_2 system for a temperature of 1600 °C. The liquidus lines (where the slags would be saturated in CaO and MgO) and the dual saturation (MgO–CaO) spot at the selected temperature are highlighted [11].

2. Experimental and calculation procedures

2.1. Thermodynamic and mass balance calculations

Firstly, thermodynamic simulations of the slag-refractory interaction at 1600 °C were performed in order to better understand the phase transformations and identify the most reactive slag composition. Based on commercial MgO–C brick designed for ladle slag lines (Magnesita Refratários S.A.), the evaluated refractory chemical composition comprised 77 wt% of MgO, 18 wt% of carbon and 5 wt% of a blend of antioxidants ($Al+Si+B_4C$). Three industrial slags presenting high reactivity (as they had low basicity, $B_3 < 1$, Eq. (2) and Table 1) were selected and two of them (X and Y) contained CaF_2 as an additional fluxing agent.

$$B_3 = \frac{CaO}{Al_2O_3 + SiO_2} \quad (2)$$

Thermodynamic simulations were carried out using FactSage™ [version 6.3.1, Thermfact/CRCT (Montreal) and GTT-Technologies (Aachen)], which comprises a series of modules that access and cross link thermodynamic databases and allow various calculations. FactPS and FToxid databases and Equilib and Viscosity modules were selected for this evaluation. All simulations were conducted considering a constant temperature of 1400 or 1600 °C and pressure of 1 atm.

An enhanced modeling simulation (previously developed by the authors [13,14]) was used in this investigation. Initially, 100 g of slag (*S*) and 100 g of the refractory (*R*) were considered in the first reaction stage between these two materials. After the first reaction step, the resulting liquid Slag (S_A) was again put in contact with the same amount (100 g) of the original refractory composition and a further calculation was carried out. This procedure was constantly repeated until the calculated amount of the main solid phases (after all the possible reactions) attained a constant value and the liquid slag was saturated (Fig. 2).

The thermodynamic simulations indicated that slag *Y* (with the lowest MgO content and higher amount of CaF_2 and FeO) should react to a greater extent with the MgO–C, leading to the refractory dissolution at high temperature. For this reason, some additional calculations aiming to predict a novel conditioned slag Y, saturated with MgO and CaO, were performed using the online software *Ladle Mass Balance/Slag Model* (Magnesita e-tech [11]). This tool uses a mathematical approach to calculate slag compositions based on the input values of the end-user. As a result, the software provided a

Table 1
Chemical composition of the industrial slags evaluated in this work (wt%).

Slag	SiO_2	FeO	MnO	Cr_2O_3	Al_2O_3	CaO	MgO	CaF_2	Basicity (B_3)
X	8.7	2.6	3.5	–	32.1	40.4	10.0	2.7	1.0
Y	62.5	4.9	–	5.9	1.5	18.2	1.1	5.6	0.3
Z	41.9	3.3	18.3	–	2.6	19.6	14.4	–	0.4

novel slag composition based on the mass balance model at the temperature of interest (1600 °C).

In order to evaluate the impact of the slag conditioning practice on the refractory wear, some corrosion tests were carried out using both slags: Y and $Y_{conditioned}$ (this latter was prepared based on the mixture of the oxide contents provided by the mass balance calculations). The details of the refractory compositions and experimental procedure selected for the corrosion analyses are described in the following section.

2.2. Experimental tests

Table 2 presents the raw materials used in the refractory formulation developed in this work. MgO–C refractory bricks were prepared considering the same chemical composition highlighted earlier in Section 2.1 [77 wt% of MgO, 18 wt% of carbon (mixture of pitch, graphite and coke derived from the phenolic resin) and 5 wt% of a blend of antioxidants (Al, Si and B_4C)]. Two refractory compositions (A1 and A2) were analyzed in the experimental tests, where the main difference between them was the MgO source (magnesia type M or L, Table 2).

During the processing procedure, firstly, a ceramic blend of electrofused MgO, flake graphite, pitch and the antioxidants was obtained. After that, liquid phenolic resin was slowly added to the ceramic compositions in order to act as a binder.

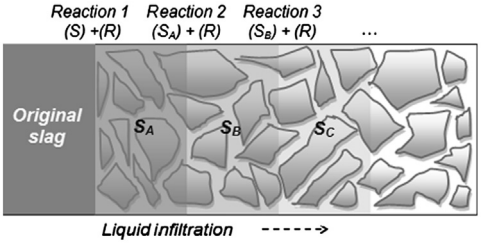

Fig. 2. Sketch of the liquid composition changes after reaction with the refractory [13].

The forming process of the MgO–C bricks (160 mm × 85 mm × 63 mm) was carried out using a hydraulic press and pressure of 200 MPa. The samples were cured at 200 °C for 6 h.

For the physical and thermo-mechanical characterization of the MgO–C refractories, the prepared bricks were cut into different sizes (according to the selected test) using a diamond saw and the attained materials were dried at 110 °C for 24 h and fired under reducing atmosphere at 1400 °C for 5 h (5 °C min^{-1}) in a refractory sealed box, where the samples were embedded in coke.

The apparent porosity of cubic samples (40 mm × 40 mm × 40 mm) after curing and firing was measured by the Archimedes method (ASTM C380-00), using querosene as the immersion liquid. The cold modulus of rupture of the materials was evaluated by uniaxial compressive strength tests (JIS R-2206 standard—samples' size: 40 mm × 40 mm × 40 mm) in MTS equipment using a 24.3 kN/min loading rate.

Hot modulus of rupture (HMOR) tests was carried out in three-point bending apparatus at 1400 °C, using prismatic samples (40 mm × 40 mm × 160 mm—ASTM C583-80). The cured and pre-fired samples were wrapped in nickel foil before testing in order to inhibit the interaction with oxygen. For each composition, three samples were evaluated. Concerning the thermal shock tests, prismatic samples (40 mm × 40 mm × 160 mm) were subjected to a total of 10 heating and cooling cycles (ASTM C1171-91). The samples were immersed in molten steel in an induction furnace at 1600 °C and kept at this temperature for 90 s. After that, they were withdrawn and cooled in air for 10 min. This procedure was considered as one full cycle. The damage caused by the thermal changes was evaluated by the elastic modulus measurements at room temperature (ultrasonic pulse technique) as a function of the thermal cycles (0, 1, 3, 5, 7, 10 cycles).

Two conventional corrosion tests (cup-test and induction furnace) were used to analyze the refractory wear. The static test (cup-test) was performed in cubic samples (40 mm × 40

Table 2
Raw materials used in the refractory compositions developed in this work.

Raw materials	Characteristics	Companies
Electrofused MgO	Type M ($CaO+SiO_2$) = 2.0 wt%, Crystal size = 1220 μm Type L ($CaO+SiO_2$) = 1.3 wt%, Crystal size = 2280 μm	Magnesita Refratários S.A. (Brazil)
Phenolic resin	H_2O = 7.6 wt% Viscosity = 5261 cP	Dynea (Brazil)
Pitch	Carbores® F Coke yield = 82.04 wt%	Rutgers (Brazil)
Graphite	Graflake® 9980 C = 99.5 wt%, Ash = 0.5 wt%	Nacional de Grafite (Brazil)
Aluminum powder	101	Alcoa Alumínio (Brazil)
Silicon powder	Silgrain	Elkem Refractories (Norway)
Boron carbide (B_4C)	$d < 45$ μm	China Brasilis (China)

mm × 40 mm) with a central inner hole of 25 mm in diameter and 25 mm depth. Before the experiments, the cup samples were filled in with 18 g of slag Y (original or conditioned compositions). The corrosion analyses were carried out in an electrical furnace (Lindberg Blue, Lindberg Corporation, USA) in air (oxygen partial pressure = 0.21 atm) at 1400 °C for 3hours. The oxidizing atmosphere was chosen for the cup tests in order to simultaneously evaluate the oxidants effectiveness and the corrosion performance. After that, the corroded samples were cut and had their cross sections polished and prepared for scanning electron microscopy analysis (SEM and EDS, Philips, XL-30 FEG model, Germany). In addition, the slag penetration area was calculated using the Image J 1.42q software (Wayne Rasband, National Institutes of Health, USA), according to the procedure described by Braulio et al. [15], in order to quantify the corrosion damage.

Additionally, the dynamic corrosion evaluation was carried out in an induction furnace at 1600 °C for 4 h, using molten metal and slag *Y* (original or conditioned composition) as corrosion agents. The furnace was lined with refractory sections and the liquid slag renewed every 30 min to keep the same slag composition and activity during the test. After the experiment, the furnace was allowed to cool to room temperature and the relative corrosion rates were analyzed.

3. Results and discussion

3.1. Thermodynamic and mass balance calculations

Fig. 3 shows the phase evolution predicted by the thermodynamic simulation after contact of the industrial slags and MgO–C refractory at 1600 °C. The first calculation step presented in these graphs represents the initial reaction between the molten liquid and the refractory components. Due to the chemical differences of the slag composition and the MgO–C refractory, and the low basicity of the former, it was expected that MgO should be readily dissolved into the liquid at high temperature. Such behavior was attained mainly for slags Y and Z, which were the ones with $B_3 < 1$ and higher SiO_2 contents. As observed in Fig. 3b and c, the dissolution of MgO resulted in a marked increase of the liquid content at the first calculation step, considering that the initial slag amount was 50 wt%. Nevertheless, the main transformation for both evaluated systems (slag Y-refractory and slag Z-refractory) seems to take place only at this first contact between liquid and solid as, from the 2nd till the 6th calculation steps, no significant changes are detected in the liquid and MgO content.

Regarding slag *X*, the lower SiO_2 content (8.7 wt%) and the higher amount of CaO in the molten phase (40.4 wt%) resulted in a less reactive liquid, as almost no MgO dissolution was detected in its first contact with the refractory (Fig. 3a and d).

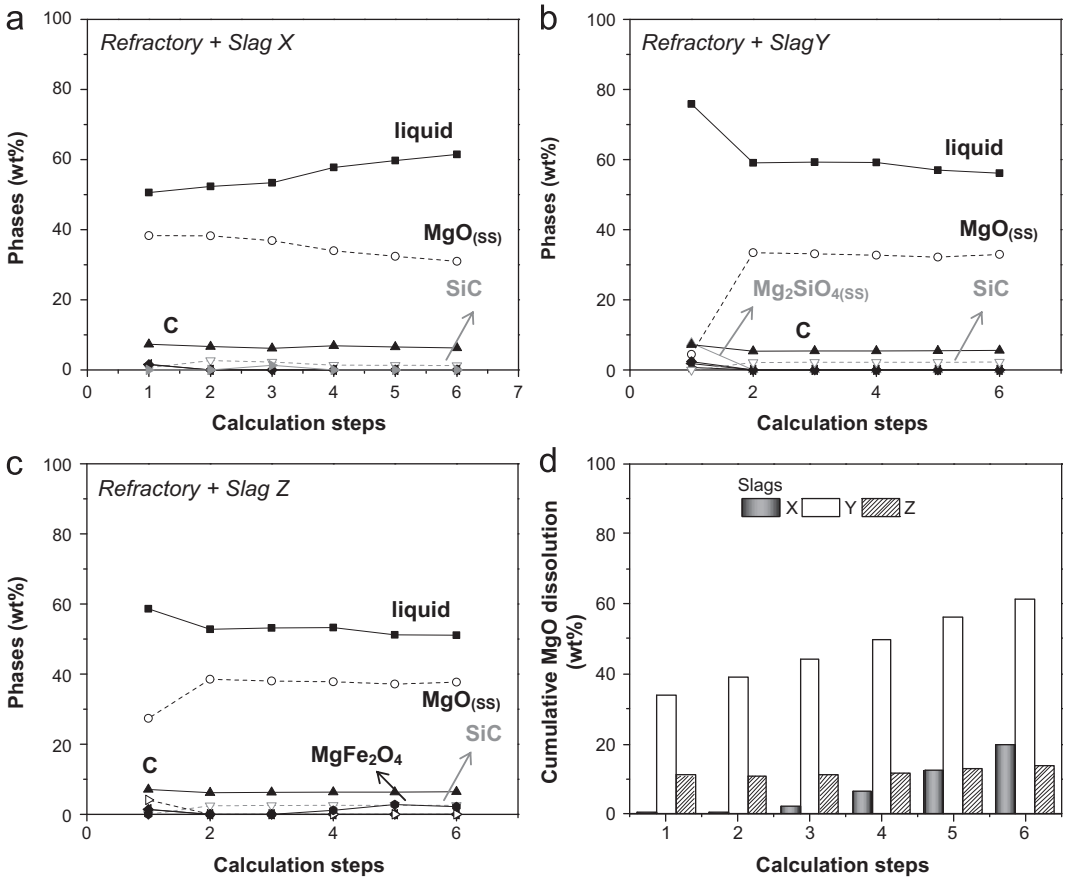

Fig. 3. Phase evolution (predicted by the thermodynamic simulations) for the MgO–C refractory and molten slags [(a) X, (b) Y and (c) Z] interaction at 1600 °C. (d) Cumulative MgO dissolution (wt%) into the slags at 1600 °C.

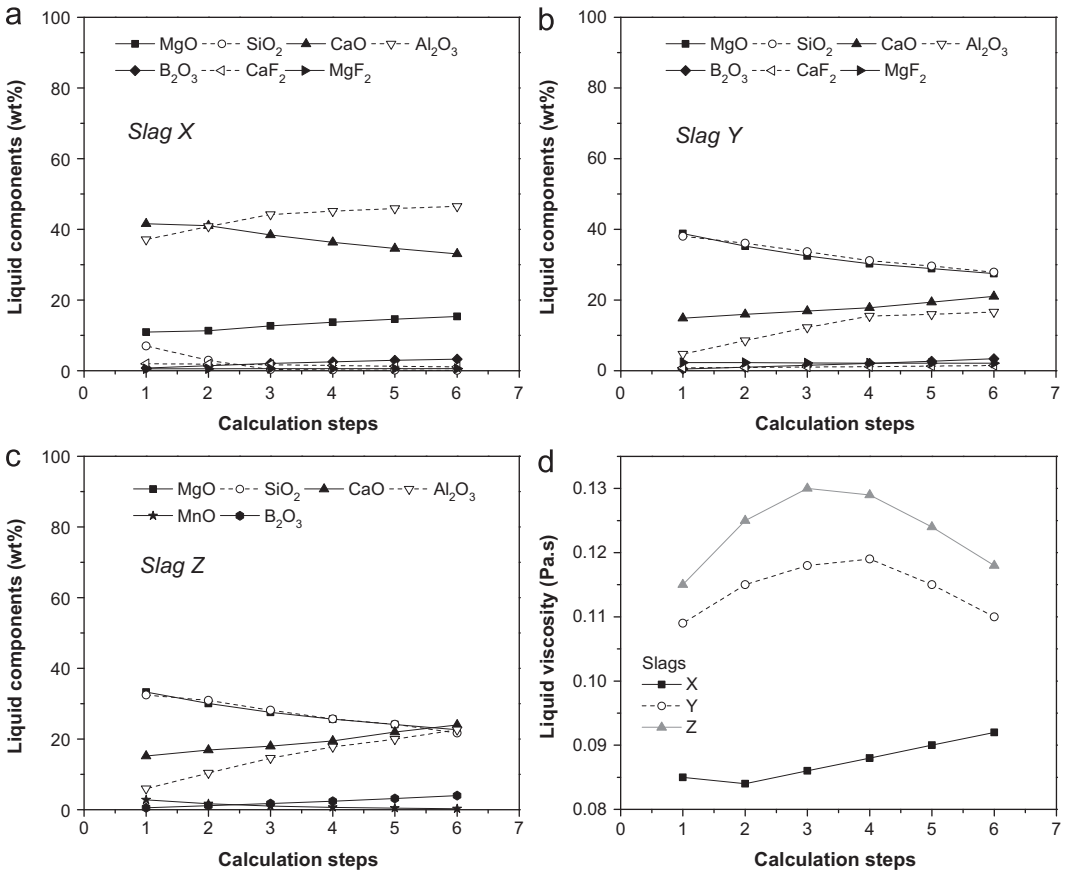

Fig. 4. Liquid composition evolution (wt%) of the slags (a) X, (b) Y and (c) Z as a function of the thermodynamic calculation steps (temperature = 1600 °C). (d) Slag viscosity after their interaction with the refractory material.

Table 3
Chemical compositions of the original and conditioned slag *Y*.

Slags (wt%)	SiO_2	FeO	MnO	Al_2O_3	CaO	MgO	CaF_2	Cr_2O_3	Basicity (B_3)
Y	62.5	4.9	–	1.5	18.2	1.1	5.6	5.9	0.3
Y conditioned	28.1	2.2	2.7	0.9	46.1	13.0	4.5	2.6	1.6

SiC, forsterite (Mg_2SiO_4) containing Ca^{2+} in solid solution and spinel ($MgFe_2O_4$) was also predicted to be formed in the slag–refractory interface as minor phases (Fig. 3). Silicon carbide should be generated by the reaction of the silicon powder (antioxidant) and the carbon sources contained in the refractory composition. On the other hand, the other antioxidants (Al and B_4C) might be oxidized and incorporated into the liquid phase at high temperature.

Despite the lower reactivity of slag *X*, the incorporation of Al_2O_3 into the liquid and, consequently, the decrease of the basicity of this phase (from 0.99 to 0.70), will allow a further dissolution of the MgO for the next calculation steps (Fig. 3a and d). The chemical composition of the resultant slags (after their interaction with the refractory components) and their viscosity are presented in Fig. 4. Slag X showed lower viscosity values, which could be associated with the reduced SiO_2 content and the presence of 2.7 wt% of CaF_2 in this composition. However, as this molten phase becomes richer in Al_2O_3 and MgO (due to the dissolution of those oxides from the refractory–calculation steps > 2) its viscosity tends to increase.

Although slag Y contained the highest SiO_2 amount (62.5 wt%) its viscosity values (after the interaction with the MgO–C refractory) were lower than the ones predicted for slag Z (Fig. 4d). It is important to highlight that this property depends on the balance among the oxide and fluorine phases contained in the liquid composition at a high temperature [2,12,14]. SiO_2, Al_2O_3 and MgO are some of the main oxides that will induce the increase of the liquid viscosity. On the other hand, FeO, MgF_2 and CaF_2 should have the opposite trend and lead to the formation of a more fluid slag [12]. Additionally, both liquids derived from slags Y and Z interactions with the refractory reached a maximum viscosity value between the 3rd and 4th calculation steps.

Considering that slag Y is the most reactive one, resulting in a greater MgO dissolution at 1600 °C (as predicted in Fig. 3d), a novel composition of this liquid (based on mass balance simulations) was calculated for further evaluation of the changes or corrosion improvements induced by the conditioning practice. Table 3 presents the original and conditioned compositions of slag Y.

Table 4
Physical and thermo-mechanical properties of the evaluated MgO–C refractories.

Properties		*Refractory A1*		*Refractory A2*	
		200ºC	**1400ºC**	**200ºC**	**1400ºC**
Apparent porosity (%)		4.85±0.59	10.21±0.12	4.90±0.93	10.45±0.08
Cold crushing strength (MPa)		29.29±2.08	32.98±4.26	27.30±1.62	27.78±1.74
Hot modulus of rupture (1400 ºC) (MPa)		12.80±1.09	12.68±0.17	13.95±3.19	12.12±0.61
Thermal shock resistance (ΔT) – Evolution of the samples' elastic modulus (GPa)	0 cycle	–	27.43±0.12	–	26.07±0.27
	1 cycle	–	11.34±0.76	–	10.99±0.43
	3 cycles	–	8.64±0.15	–	9.11±1.64
	5 cycles	–	5.83±0.71	–	7.17±2.39
	7 cycles	–	4.44±0.31	–	5.51±2.96
	10 cycles	–	–	–	3.27±2.38

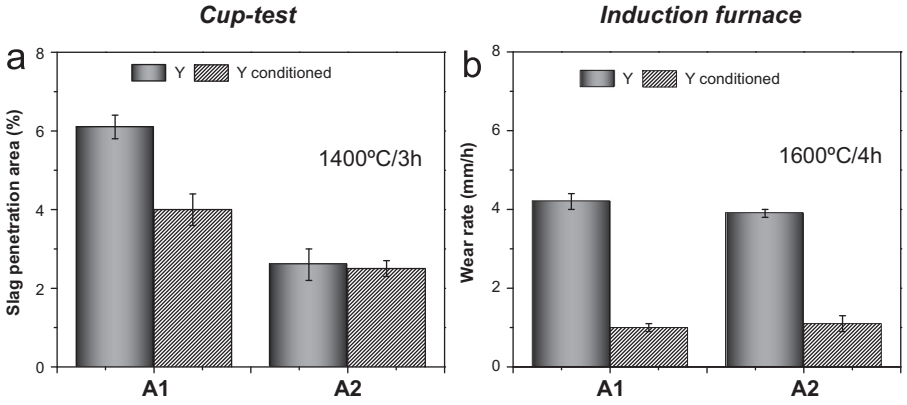

Fig. 5. (a) Slag penetration area (%) and (b) wear rate of the MgO–C refractory compositions after the corrosion resistance tests.

Table 5
Predicted phases to be found at 1400 ºC at the first slag + refractory A1 contact.

Phases (wt%)	**Slags**	
	Y	***Y* conditioned**
Liquid[*]	42.5	37.9
Mg_2SiO_4	41.0	–
$MgO_{(ss)}$	3.7	41.6
$MgAl_2O_{4(ss)}$	0.8	–
C	7.2	7.2
Cr_3C_2	2.3	1.0
FeSi	1.8	1.3
Fe_3C	0.8	–
Ca_2SiO_4	–	9.3
MnSi	–	1.2
SiC	–	0.5

[*]MgO content in the Liquid: $Y = 38$ wt% and Y cond. = 9 wt%.

The conditioned slag Y was saturated with CaO and MgO. Therefore, the major changes in the novel composition were the increase of those oxide contents and decrease of SiO_2, FeO and CaF_2 amounts. Those changes resulted in a significant increase of the slag basicity (~5.7 times higher than the original liquid Y), which may induce a better compatibility between the basic MgO–C refractory and the slag, reducing the corrosion wear.

3.2. Physical and thermo-mechanical properties of the MgO–C refractories

Two MgO–C brick compositions were prepared and the only difference between them was the MgO source used (Table 2): refractory A2 contained electrofused magnesia with higher purity and larger crystal size ($d = 2280$ μm).

In order to investigate the effect of the quality of this raw material in the refractory properties, some mechanical tests (at room and high temperature), apparent porosity and thermal shock measurements were carried out using samples attained after curing (200 °C/6 h) and firing (1400 °C/5 h under reducing atmosphere). The results of these experiments are shown in Table 4.

As pointed out in the literature [16], the chemical transformations of carbon-based binders (pitch and organic resins) may directly affect the refractory properties, with new carbon bonds forming at the first heating treatment. Nevertheless, when comparing the hot mechanical strength and thermal shock results of the samples A1 and A2 (Table 4), no statistical differences were identified between the attained values. Moreover, despite the carbon yield due to the pitch and the phenolic resin binders, the apparent porosity of both evaluated materials increased after the firing treatment at 1400 °C, which should be related to the release of the volatile carbon containing species that were generated at a high temperature.

Concerning the samples´ ability to withstand the stress generated by sudden temperature changes, it was observed that both compositions presented a continuous decrease in the elastic modulus values as a function of the thermal cycles. Although the MgO–C samples did not show visible cracks on their surfaces after 10 cycles, it was not possible to measure the E values for composition A1 using the ultrasonic pulse technique. Based on the results presented in Table 4, the use of a magnesia source with higher quality in composition A2 did not lead to major changes in the MgO–C refractory thermo-mechanical behavior. Hence, in order to better evaluate the viability of using such raw material, some additional corrosion tests were carried out considering the original and conditioned slag *Y*.

3.3. Corrosion behavior and microstrutural analysis

Static (cup-test) and dynamic (induction furnace) corrosion tests were performed at 1400 °C and 1600 °C, respectively, and the slag penetration area and wear rate of the samples are shown in Fig. 5.

The corrosion cup-tests present the drawbacks associated with static procedures, i.e., no temperature gradient, rapid saturation of slag composition with reaction products and no slag flow [17]. Nevertheless, it is simple as many samples can be analyzed in a short time and the results can be better correlated with the thermodynamic calculations. According to Fig. 5, as expected, the original slag *Y* (acid slag, $B_3 = 0.28$) led to higher penetration of the liquid into the refractory microstructure.

Furthermore, based on the static corrosion results (Fig. 5a), the benefits from the slag conditioning practice (to induce a better compatibility between refractory and molten liquid) were mainly detected for sample A1, with an increase close to 34% of the refractory corrosion resistance when the measurements were carried out with slag *Y* conditioned. On the other hand, samples A2 (comprised by an MgO source of higher purity) presented a similar corrosion behavior in contact with both evaluated slags, and the liquid infiltrated areas were roughly two times lower than the ones calculated for the refractory A1.

Some metal and slag circulation is observed in the induction furnace test. Moreover, a temperature gradient can be established and higher corrosion usually takes place at the melt/slag line. Due to these features, some authors stated that the results of such corrosion tests can better simulate the refractory wear in a practical ladle furnace [5,17]. The samples in contact with the steel-conditioned slag presented lower corrosion rates (Fig. 5b) and, in this case, the use of different MgO sources in the refractory compositions seems to be irrelevant to the wearing rate of such materials (as samples A1 and A2 showed similar wear after interaction with slag Y and slag Y conditioned). Thus, based on these results, one good alternative for the refractory producers should be: (1) the use of a raw material of lower cost (i.e., MgO type M, Table 2, presenting higher CaO and SiO_2 content as impurity) in the MgO–C

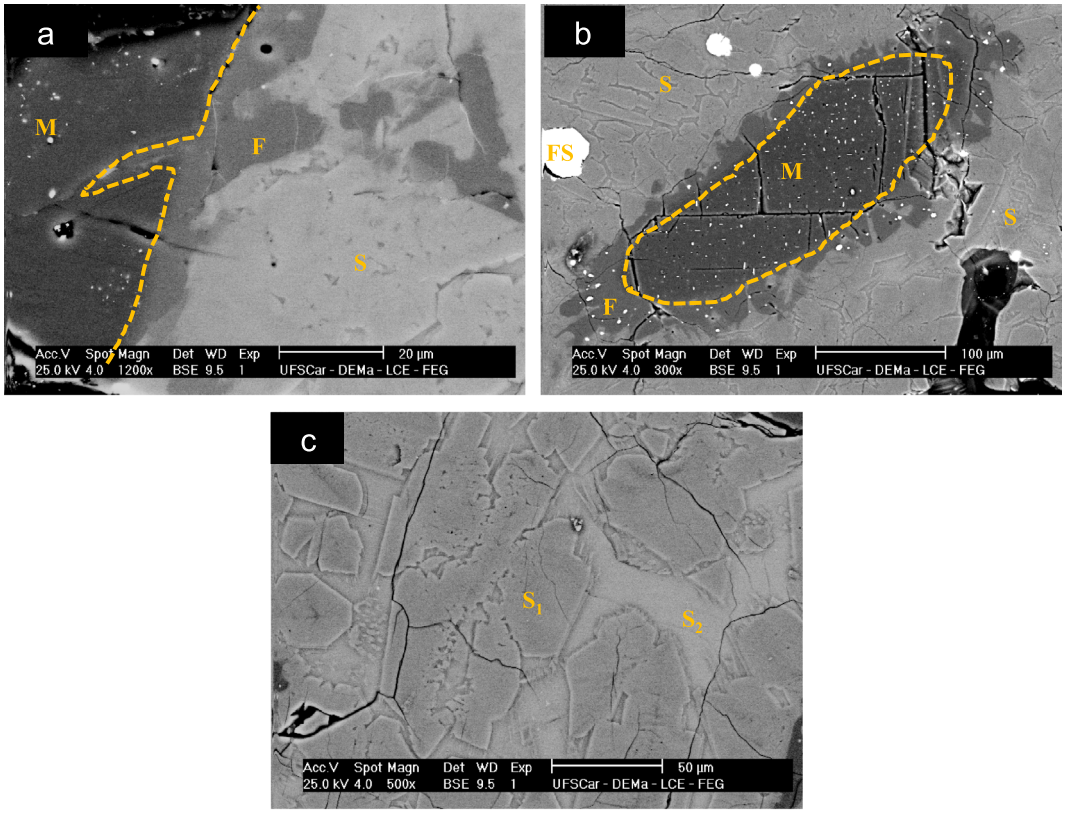

Fig. 6. A1 corroded samples after contact with slag Y (corrosion cup test) at 1400 °C for 3 h. (a) refractory–liquid interface, (b) and (c) slag region. M = MgO, S = slag, F = forsterite (Mg_2SiO_4), FS = FeSi, $S_1 = CaMgSi_2O_6$, S_2 = anorthite ($CaAl_2Si_2O_8$).

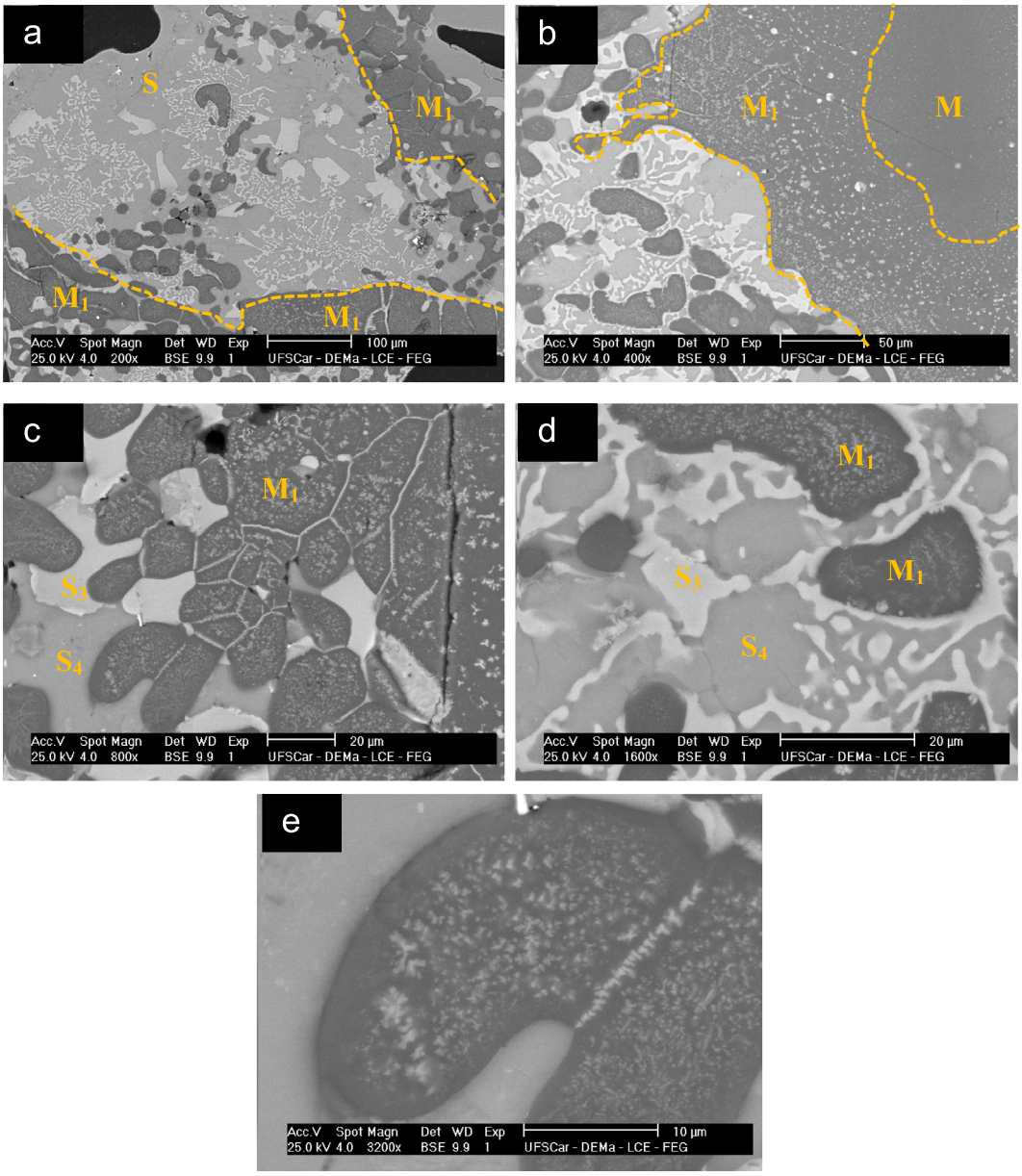

Fig. 7. A1 corroded samples after contact with slag Y conditioned (corrosion cup test) at 1400 °C for 3 h. (a–c) refractory–liquid interface, (d) slag region and (e) image highlighting the MgO grains containing MnO and Fe_2O_3 in its structure. M = MgO, S = slag, M_1 = MgO + MnO, S_3 = mixture of MnO + MgO + Fe_2O_3 + CaO + Al_2O_3, and S_4 = CaO + SiO_2.

compositions, combined with (2) the slag conditioning practices in the ladle refining process in order to reduce costs and the chemical attack of the refractory lining.

The cross section area of the corroded sample A1 (attained after the cup-test) was analyzed using SEM and EDS techniques. It was chosen to only evaluate the microstructure of refractory A1 as this composition showed distinct corrosion behavior when in contact with the two tested slags. Additionally, some thermodynamic simulations of the first contact between refractory and slags (Y and Y conditioned) were also carried out considering the temperature of 1400 °C (Table 5).

Considering an equilibrium condition, the dissolution of MgO from the refractory and its further reaction with $SiO_{2(l)}$ from slag Y should mainly give rise to forsterite (Mg_2SiO_4) formation at 1400 °C. Some minor phases are also predicted to be formed at a high temperature, such as $MgAl_2O_4$, Cr_3C_2, FeSi and Fe_3C. Analyzing the microstructure of the corroded A1 sample, the presence of forsterite at the solid-slag Y interface was confirmed (Fig. 6a). Furthermore, as highlighted in Fig. 6b, some loose grains of MgO were also found completely immersed in the slag region showing a continuous Mg_2SiO_4 layer on their surface. After cooling, the molten slag (enriched in the refractory components) seems to segregate into two different phases, $CaMgSi_2O_6$ and anorthite ($CaAl_2Si_2O_8$), as pointed out by EDS analysis (Fig. 6c).

On the other hand, the changes in the chemical composition of slag Y after the conditioning procedure (CaO and MgO saturated) led to different phase transformations, with the

prediction of Ca_2SiO_4 generation and some other minor phases (Cr_3C_2, FeSi, Fe_3C, SiC and MnSi) as shown in Table 5. The thermodynamic calculation results also strengthen the lower corrosion of the A1 samples after the interaction with the conditioned slag, due to the higher MgO amount and lower liquid content predicted to be found at 1400 °C.

Fig. 7 presents the images of the MgO–C corroded samples after contact with the conditioned slag Y.

Some differences between the simulations and experimental results were observed, as no Ca_2SiO_4 crystals were clearly identified in the corroded microstructure. When analyzing the slag region (Fig. 7a and d), two distinct phases could be detected where S_3 (light gray phase with irregular morphology) consisted of a mixture of $MnO+MgO+Fe_2O_3+CaO+Al_2O_3$, and S_4 (continuous gray phase) comprises only $CaO+SiO_2$ in its composition.

The MgO grains located close to the reaction interface incorporated around 10 wt% Mn and 1 wt% Fe into their composition, resulting in the presence of small crystals (region/grains highlighted as M_1, Fig. 7b–e) in their structure. As shown in Fig. 7b, only the outer region of the coarser MgO grains was enriched in Mn and Fe (M_1), and pure magnesia could still be identified (M) in some areas. Nevertheless, no slag attack of the MgO grains could be observed, reinforcing the importance of controlling the slag composition (by implementing the conditioning practices) in order to improve the corrosion resistance of refractory materials at high temperature.

4. Conclusions

Based on the results presented in this work, it can be concluded that thermodynamic and mass balance calculations are good tools to be used in the evaluation of slag-refractory compatibility and to predict phase transformations at a high temperature. The change of the chemical composition of a slag (in order to attain a MgO and CaO saturated liquid) can inhibit the slag attack. When comparing the corrosion behavior of two MgO–C containing distinct magnesia sources, it was attested that the conditioning practice was more effective to enhance the refractory corrosion resistance than the use of a high quality (higher purity) raw material. Nevertheless, it must be pointed out that the wear rate of the refractory bricks containing coarser and higher quality MgO source was still slightly better. Therefore, proper slag engineering can be a suitable replacement for purchased synthetic slags and the conditioning practices can directly improve refractory life, with more competitive costs for the refractory producer and end-user.

Acknowledgments

The authors are grateful to CNPq, FIPAI and Magnesita Refratários S.A. for supporting this work.

References

[1] E. Pretorius. Slag fundamentals. In: An Introduction to the Theory and Practice of EF Steelmaking, Iron & Steel Society Short Course Book. New Orleans, USA, 1998, p. 1–38.
[2] E.B. Pretorius, R.C. Carlise, Foamy slag fundamentals and their practical application to electric furnace steelmaking, in: Proceedings of the 56th Electric Furnace Conference, ISS-15-18, New Orleans, USA, 1998, p. 275–291.
[3] R. McClanahan, L. Kibler, L. Wolfe, A.C. Dyar, J.M. Compton. Comparative analysis of dolomitic lime and Chinese magnesite practices in electric arc furnace steelmaking slags, Technical Paper, 2003. Available from: ⟨http://www.carmeusena.com/files/files/techpapersreports/nsbhp_20paper_aise_202003⟩.
[4] M.M. Rahman. Fundamental investigation of slag/carbon interactions in electric arc furnace steelmaking process, thesis, Materials Science and Engineering. University of New South Wales, 2010, p. 1–230.
[5] T.A. Ávila, R.S. Freire, G.F.B.L. Silva, R.N. Borges. Design of slags compatible with refractory systems, in: Proceedings of Unified International Technical Conference on Refractories, UNITECR 2009, Salvador, Brazil, 2009, p. 1–4.
[6] K.S. Kwong, J.P. Bennet, Recycling practices of spent MgO–C refractories, Journal of Minerals and Materials Characterization and Engineering 1 (2) (2002) 69–78.
[7] S. Jansson, A study on molten steel/slag/refractory reactions during ladle steel refining, thesis, Royal Institute of Technology, Stockholm, Sweden; 2005. p. 1–32.
[8] L.C. Oertel, A. Costa e Silva, Application of thermodynamic modeling to slag-metal equilibra in steelmaking, Calphad 23 (3–4) (1999) 379–391.
[9] S. Surinder, P. Ghag, P.C. Hayes, H.G. Lee, Physical model studies on slag foaming, ISIJ International (Japan) 38 (11) (1998) 1201–1207.
[10] A.P. Luz, T.A. Ávila, P. Bonadia, V.C. Pandolfelli, Slag foaming: Fundamentals, experimental evaluation and application in the steelmaking industry, Refractory World Forum 3 (2) (2011) 91–98.
[11] Ladle Mass Balance/Slag Model, Magnesita e-tech. Available from: ⟨http://etech.lwbref.com/Applications/Ladle/ladleMassBalance.aspx?Mode=Preview⟩.
[12] E. Andersson, D. Sichen, The effect of CaF2 in the slag in ladle refining, Steel Research International 80 (8) (2009) 544–551.
[13] A.P. Luz, A.G. Tomba Martinez, M.A.L. Braulio, V.C. Pandolfelli, Thermodynamic evaluation of spinel containing refractory castables corrosion by secondary metallurgy slag, Ceramics International 37 (2011) 1191–1201.
[14] A.P. Luz, M.A.L. Braulio, A.G. Tomba Martinez, V.C. Pandolfelli, Slag attack evaluation of in situ spinel-containing refractory castables via experimental tests and thermodynamic simulations, Ceramics International 38 (2012) 1497–1505.
[15] M.A.L. Braulio, A.G. Tomba Martinez, A.P. Luz, C. Liebske, V.C. Pandolfelli, Basic slag attack of spinel-containing refractory castables, Ceramics International 37 (2011) 1935–1945.
[16] B. Rand, B. McEnaney, Carbon Binders from polymeric resins and pitch Part I—Pyrolysis behavior and structure of the carbons, Transactions and Journal of the British Ceramic Society 84 (1985) 157–165.
[17] W.E. Lee, S. Zhang, Melt corrosion of oxide and oxide–carbon refractories, International Materials Reviews 44 (3) (1999) 77–104.